





# The Effect of Feedback Control on the Onset of Surface-Tension Driven Convection with the Internal Heat Generation: An Analytical Approach

Agrahara Sanjeevmurthy Aruna <sup>1,\*</sup>, Tumbadi Veerananjappa Karnakumar <sup>2</sup>, Doddaballapur Lakshminarayana Shivaraj Kumar <sup>1</sup>, Girish Sharma <sup>2</sup>

<sup>1</sup> Department of Mathematics, Ramaiah Institute of Technology, Bengaluru-560054, India; arunas@msrit.edu (A.S.A), dlshivaraj@gmail.com (L.S.K);

<sup>2</sup> Department of Mathematics, KLE S. Nijalingappa College, Bengaluru-560010, India; karnakumar663@gmail.com (T.V.K), girishsharma1996@gmail.com (G. S);

\* Correspondence: arunas@msrit.edu (A.S.A)

Scopus Author ID 57214818606

Received: 24.05.2022; Accepted: 21.06.2022; Published: 20.11.2022

**Abstract:** An analytical study of the effect of control and internal heat generation on the onset of Surface-tension driven convection so-called Marangoni-Benard convection in the horizontal layer of fluid with temperature gradient, is studied in the problem. The resulting eigenvalue problem is thus solved using the analytical method to derive an expression for the Marangoni number. It is found that the effect of control and internal Rayleigh number influence the onset of convection. It is also demonstrated here that the onset of Surface-tension driven convection with the uniform internal heat source can be suppressed through control. Tabulation of critical Marangoni numbers is obtained for different parametric influences.

**Keywords:** surface-tension driven convection; uniform heat source; feedback control; Benard-Marangoni convection; Crispation number.

© 2022 by the authors. This article is an open-access article distributed under the terms and conditions of the Creative Commons Attribution (CC BY) license (<https://creativecommons.org/licenses/by/4.0/>).

## 1. Introduction

The Effect of Buoyancy-driven convection or surface tension-driven convection can become a major mechanism for driving a possible convective instability for a horizontal fluid layer heated from below and cooled from above. The Buoyancy-driven convection, so-called Rayleigh-Benard convection, is extensively investigated in the literature. Many studies demonstrate that the onset of convection is delayed or controlled by making use of some external mechanism, such as a magnetic field (see Ramachandramurthy *et al.* [1], Aruna [2], and Chandrasekhar [3]). All these studies demonstrated the effect of a magnetic field in electrically conducting Newtonian liquids and came to know that the magnetic field has a strong stabilizing effect. The instability of convection-driven due to the surface tension is popularly known as the Marangoni convection. In contrast, the instability caused due to the combined effects of thermal Buoyancy and surface tension is called the famous Benard-Marangoni convection. Pearson [4] was the first person to study the theoretical investigation of Marangoni-Benard convection by performing linear stability analysis by considering an infinite fluid layer of some finite depth, which is so small with no-slip boundary at the bottom and zero gravity. He obtained the critical Marangoni number value,  $M_c = 79.607$ , and the

critical wave number,  $a_c = 1.99$  and showed that when the Marangoni number exceeds its critical value without buoyancy force, the thermocapillary forces can cause convection. In the above Marangoni-Benard instability analysis, the convective instability is induced by the temperature gradient, decreasing linearly with fluid layer height. The heat source is an important mechanism to enhance convection in a chemical reaction. The studies by Sparrow *et al.* [5] and Roberts [6] demonstrate that internal heat generation creates nonlinear temperature distribution across fluid layers due to thermal instability in a horizontal fluid layer of Newtonian liquids. The effect of a quadratic basic state temperature profile caused by internal heat generation was first addressed by Char and Chiang [7] for Benard-Marangoni convection. Later, Wilson [8] investigated the effect of the internal heat generation on the onset of Marangoni-Benard convection when the lower boundary is conducting and insulating to temperature perturbations. He found that the effect of increasing the internal heat generation is always destabilizing the system.

However, similar mechanisms, such as variable heat source, magnetic field, etc., are applied to control the onset of convection, but literature feedback control is very scarce. This study illustrates a sincere attempt to suppress the onset of instability due to convection by applying the feedback control mechanism. The objective of the control mechanism is to suppress the onset of convection [9] while maintaining a conduction state in the fluid layer. Tang and Bau [10,11] and Howle [12] presented their work on the onset of Buoyancy driven convection and showed that the critical Rayleigh number for the onset of Rayleigh-Benard convection can be suppressed due to the control. Or *et al.* [13] analytically demonstrated that the use of control strategies to stabilize long-wavelength instabilities occurs in the Marangoni-Benard convection problem.

Furthermore, Bau [14] has shown independently how such control can delay the onset of Marangoni-Benard convection on a linear basis with no-slip boundary conditions at the bottom. Recently, Arifin *et al.* [15] have shown that control can delay the onset of Marangoni-Benard convection with free-slip boundary conditions at the bottom. A good number of recent articles [16-33] contribute to the literature pertaining to the surface tension-driven Marangoni convection and heat transfer. Therefore, this paper uses a linear controller to delay the onset of Marangoni-Benard convection in a fluid layer with uniform internal heat generation. Here we first transformed a set of coupled partial differential equations into a system of ordinary nonlinear equations using the normal mode analysis technique. Here, we first derived the analytical expressions for the thermal Marangoni number. Next, we demonstrate how one can control the no-motion state, the conduction to convection state, in the Marangoni-Benard convection problem. Here we utilized uniform internal heat generation as the main mechanism to suppress the onset of convection for a particular choice of parameter values.

## 2. Materials and Methods

### 2.1. Formulation of the problem.

Consider an infinitely extended horizontal Newtonian fluid layer of depth  $d$  with the lower boundary being rigid isothermal and the upper boundary being free. The lower and the upper boundary are maintained at different temperatures  $T_1$  and  $T_0$ , where  $T_1 > T_0$  as shown in the adjacent figure. Let us assume that the density and dynamic viscosity are temperature-dependent. A uniform heat source is considered, and it is not temperature dependent. The upper

layer of the fluid is exposed to a positive gas having constant pressure  $P_0$  and the constant temperature  $T_0$  as shown in figure 1.

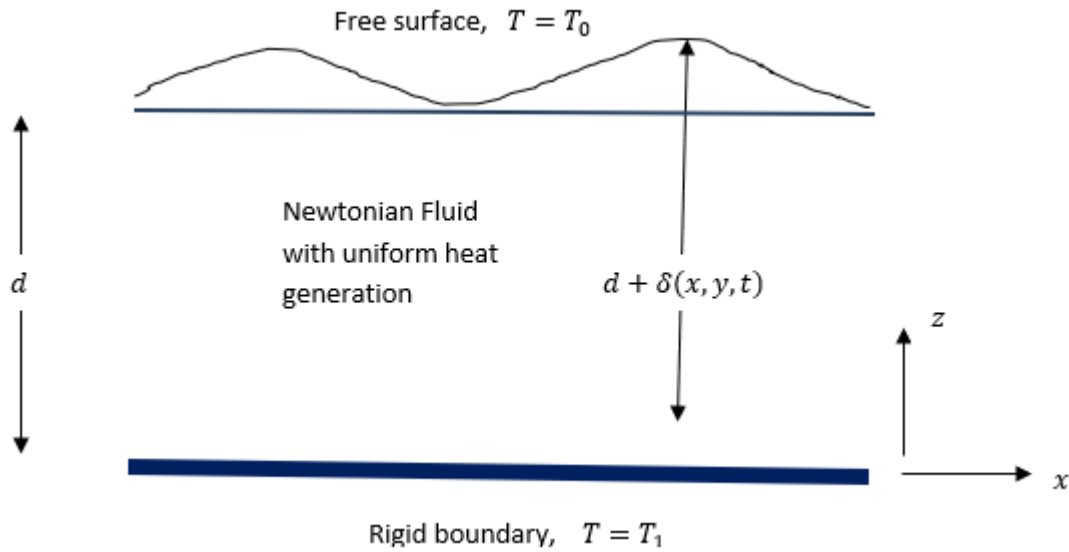


**Figure 1. Schematic of Flow Configuration**

A Cartesian frame of reference is considered so that  $x$ -axis is the bottom of the fluid layer, and  $z$ -axis is vertically directed toward the free surface. We now assume the Surface-tension  $\tau$  is a linear function of temperature gradient  $T - T_0$  according to the following relation.

$$\tau = \tau_0 - \gamma(T - T_0), \quad (2.1)$$

where  $\tau_0$  is the reference value of Surface-tension at the temperature  $T = T_0$  and  $\nu$  be the kinematic viscosity of the Newtonian fluid, which is positive for most of the fluid. The density of the fluid is a linear dependence of temperature as defined by the following relation.

$$\rho = \rho_0(1 - \alpha(T - T_0)), \quad (2.2)$$

where  $\alpha$  be the coefficient of thermal expansion of the fluid and  $\rho_0$  is the reference density when the temperature  $T = T_0$ .

The fluid considered in this problem is incompressible Newtonian; the Basic governing equations of the flow are given by

$$\nabla \cdot \vec{u} = 0, \quad (2.3)$$

$$\rho \left( \frac{\partial \vec{u}}{\partial t} + (\vec{u} \cdot \nabla) \vec{u} \right) = -\nabla p + \nu \nabla^2 \vec{u}, \quad (2.4)$$

$$\frac{\partial T}{\partial t} + (\vec{u} \cdot \nabla) T = -\kappa(\nabla^2 T) + q. \quad (2.5)$$

where  $\vec{u} = u_1 \hat{i} + u_2 \hat{j} + u_3 \hat{k}$  be the velocity vector,  $T$  is the temperature of the fluid at some point in time,  $p$  is the pressure,  $\nu$  is the kinematic viscosity,  $\kappa$  is the thermal diffusivity, and  $q$  represents uniformly distributed volumetric heat source. When the temperature exceeds its critical value, the conduction state turns out to be convective; that is, the conductive state gets distracted, and convection sets in. When the temperature gradient is large enough, the motion of the fluid occurs. Consequently, the upper free surface gets disturbed and deformable with the position of the fluid at  $z = d + f(x, y, t)$ . At the upper free surface, we have the usual kinematic conditions and continuity conditions for the normal and tangential stress. In this situation, the temperature of the fluid at the top obeys Newton's law of cooling so that the following equation holds

$$k \frac{\partial T}{\partial \hat{n}} = h(T - T_\infty).$$

where  $k$  and  $h$  are thermal conductivity and the heat transfer coefficient between the free surface and the air. The  $\hat{n}$  represents the unit outward normal to the surface. Also, we assume the boundary condition at the bottom,  $z = 0$  are no-slip and thermally conducting concerning the variation of temperature.

In order to perform linear stability analysis, it is convenient to non-dimensionalize equations (2.3) to (2.5) and also the boundary conditions using the quantities length by  $d$ , velocity by  $k/d$ , time by  $d^2/k$  and temperature gradient by  $\Delta T$ . Furthermore, during the non-dimensional process, the following eigenvalues are obtained:

$$\begin{aligned}
 M &= \frac{v\Delta T}{\rho_0 K v}, \text{ the Marangoni number} \\
 B_t &= \frac{hd}{K}, \text{ the Biot number} \\
 B_0 &= \frac{\rho_0 g d^2}{\tau_0}, \text{ the Bond number} \\
 P_r &= \frac{v}{K}, \text{ the Prandtl number} \\
 C_{rt} &= \frac{\rho_0 v K}{\tau_0 d}, \text{ the Crispation number} \\
 Q &= \frac{q d^2}{2K\Delta T}, \text{ the internal Rayleigh number.}
 \end{aligned}$$

As discussed in Bau [2], the sensors and actuators are continuously distributed, and each sensor directs an actuator installed directly beneath at the same  $(x, y)$  location. The sensors detect the deviation of the fluid state from the no-motion state to the motion state. Therefore, the acuter modifies the heated temperature as

$$T(x, y, 0, t) = \frac{1+B_i}{B_i} - K(T(x, y, 1, t) - \frac{1}{B_i}) \tag{2.6}$$

where  $K$  is the control parameter. Further, the above equations can be systematically written as

$$T'(x, y, 0, t) = -K(T'(x, y, 1, t)) \tag{2.7}$$

where  $T'$  be the deviation of the temperature of the fluid from a no-motion state to a convective state. Having  $K$ , one could be able to control the onset of convection.

### 2.1.1. Linearized problem.

To study linear stability analysis, we need to perturb any physical quantity  $\phi(x, y, z, t)$  so that

$$\phi(x, y, z, t) = \phi_0(x, y, z) + \phi(z)e^{i(\alpha_x x + \alpha_y y) + st} \tag{2.8}$$

Where  $\phi_0$  is the reference value in the basic state,  $a = \frac{(\alpha_x^2 + \alpha_y^2)}{2}$  is the horizontally averaged wave number,  $\delta$  the disturbance produced due to perturbation, and  $s$  is the complex growth rate of instability with its real part representing its frequency. At the marginal state, the imaginary part represents the frequency of amplitude.

It is now clear that the onset of instability in the growth rate  $s$  of infinitesimal perturbation is zero, and the real part of  $s$ ,  $Re(s) < 0$  represents stable mode with  $Re(s) > 0$  represent unstable modes.

Substitute the above equation into the linearized version of the equation [2.3] to [2.5], and using a standard generalized procedure, the following set of ordinary differential equation are obtained.

$$\frac{d^4 w}{dz^4} - 2a^2 \frac{d^2 w}{dz^2} + a^4 w = 0, \tag{2.9}$$

$$\frac{d^2T}{dz^2} - a^2T = -w, \tag{2.10}$$

$$\frac{d^2C}{dz^2} - a^2C = -w, \tag{2.11}$$

Subject to the following boundary conditions,

$$w(1) = 0, \tag{2.12}$$

$$(C_{rt} + C_{rs}) \left( \frac{d^3w(1)}{dz^3} - 3a^2 \frac{dw}{dz} \right) = a^2(a^2 + B_0)f, \tag{2.13}$$

$$\frac{dT(1)}{dz} + B_T T(1) = B_r f, \tag{2.14}$$

$$\frac{dC(1)}{dz} + B_S C(1) = B_s f, \tag{2.15}$$

$$w(0) = 0, \tag{2.16}$$

$$\frac{dw(0)}{dz} = 0, \tag{2.17}$$

$$T(0) + K_t T(1) = 0, \tag{2.18}$$

$$C(0) + K_s C(1) = 0, \tag{2.19}$$

$$\frac{d^2w}{dz^2} - a^2w + a^2M_t(T(1) - f) + a^2M_s(C(1) - f) = 0. \tag{2.20}$$

On the lower rigid boundary  $z = 0$ , Here, the variable  $W$  denotes the vertical velocity component,  $T$  is the temperature variation w.r.t  $z$ -axis, and  $f$  denotes the magnitude of the surface deflection of the linear perturbation to the basic quiescent state with the horizontally averaged wave number ‘ $a$ ’ in the  $xy$ -plane and the complex growth rate.

### 3. Results and Discussion

It is now clear that the differential equation, along with boundary conditions equations (2.9) to (2.20), are all coupled, and the solution of the equations is obtained analytically by performing mathematical calculations. Thus we obtained the following expression for the Marangoni number ( $M$ ) as a function of different parameters’ involved in these equations.

It is now clear that the analytical expression obtained for the Marangoni number is for the onset of Benard-Marangoni convection is a function of a wave number  $a$ , the effective crispation number  $C_{eff} = C_{rs} + C_{rt}$ , Control parameters  $K_s, K_t$  and also the  $B_0$  and  $B_T$ .

$$M = \frac{8a(a^2+B_0)(\text{SinhaCosha}-a)}{f_1} - \frac{M_s f_2}{f_1}, \tag{3.1}$$

where,

$$f_1 = \frac{(a^2 + B_0)(\text{Sinh}^3 a - a^3 \text{cosha}) + 8a^5 C_{eff}(\text{Cosha} + K_s)}{a \text{cosha} + B_T \text{sinha} + a K_s},$$

$$f_2 = \frac{(a^2 + B_0)(\text{Sinh}^3 a - a^3 \text{cosha}) + 8a^5 C_{eff}(\text{Cosha} + K_t)}{a \text{cosha} + B_T \text{sinha} + a K_t}.$$

Where  $C_{eff} = C_{rs} + C_{rt}$  called effective Crispation number. As a trivial case, it is essential to cross-verify the analytical expression of  $M$ . It is clear that when we set constant  $K_t = 0 = K_s$ , the expression of  $M$  reduced to the expression in Wilson [8], and when we set  $Q$  also 0, the expression is reduced as Bau [14].

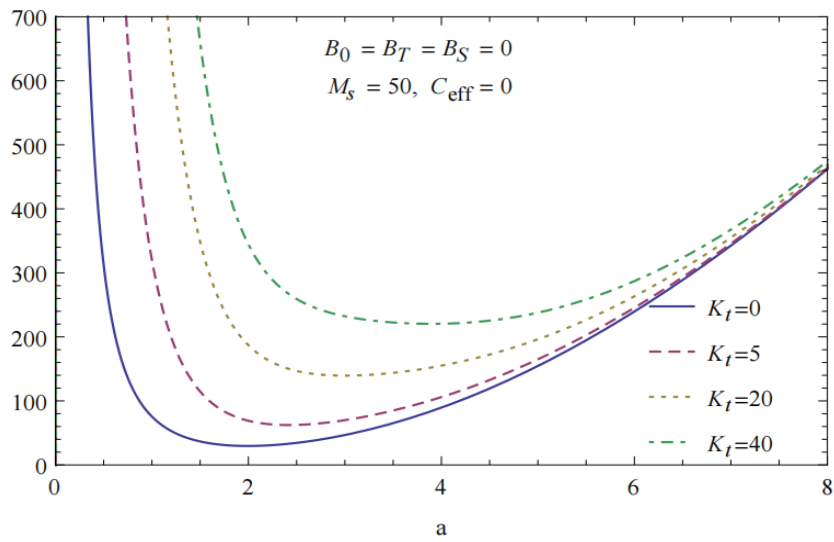


**Figure 2.** Numerically calculated Marangoni number versus the wave number ( $M_s = 50, C_{eff} = 0$ ).

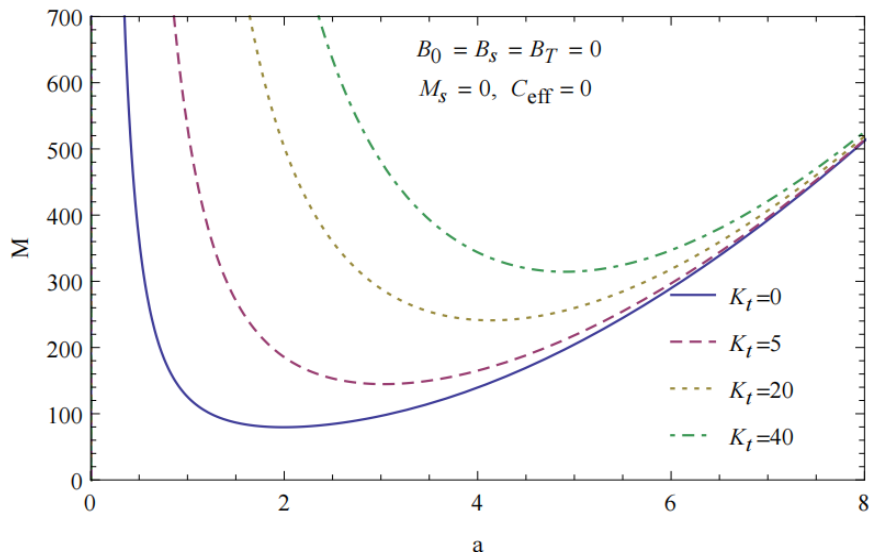


**Figure 3.** Numerically calculated Marangoni number versus the wave number ( $M_s = 0, C_{eff} = 0$ ).

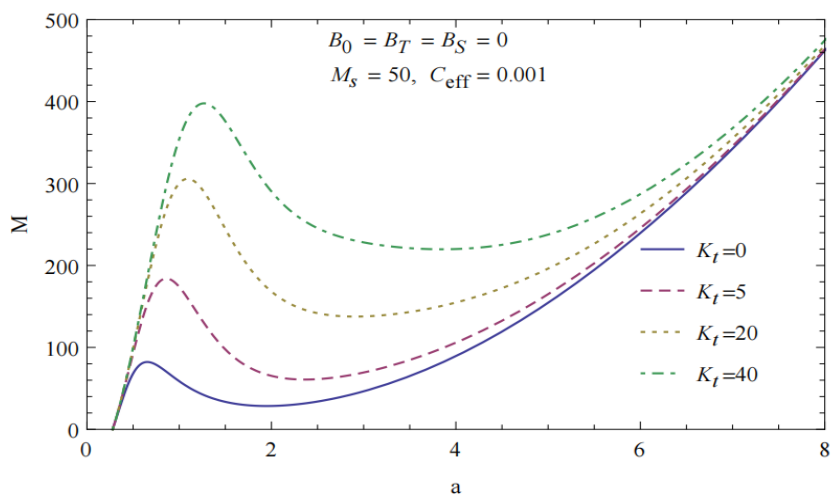


**Figure 4.** Numerically calculated Marangoni number versus the wave number ( $M_s = 50, C_{eff} = 0.001$ )

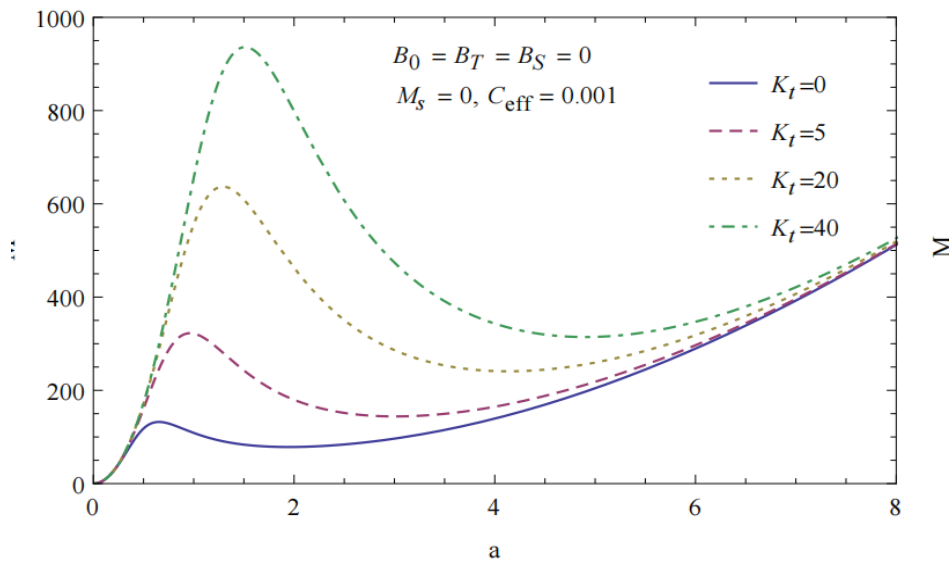


**Figure 5.** Numerically calculated Marangoni number versus the wave number ( $M_s = 0, C_{eff} = 0$ ).

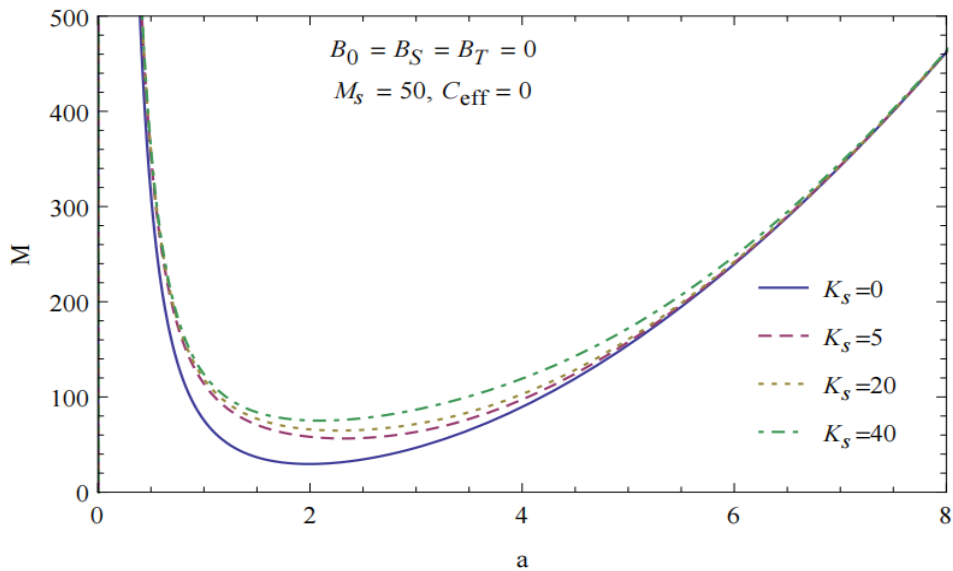


**Figure 6.** Numerically calculated Marangoni number versus the wave number ( $M_s = 50, C_{eff} = 0$ ).

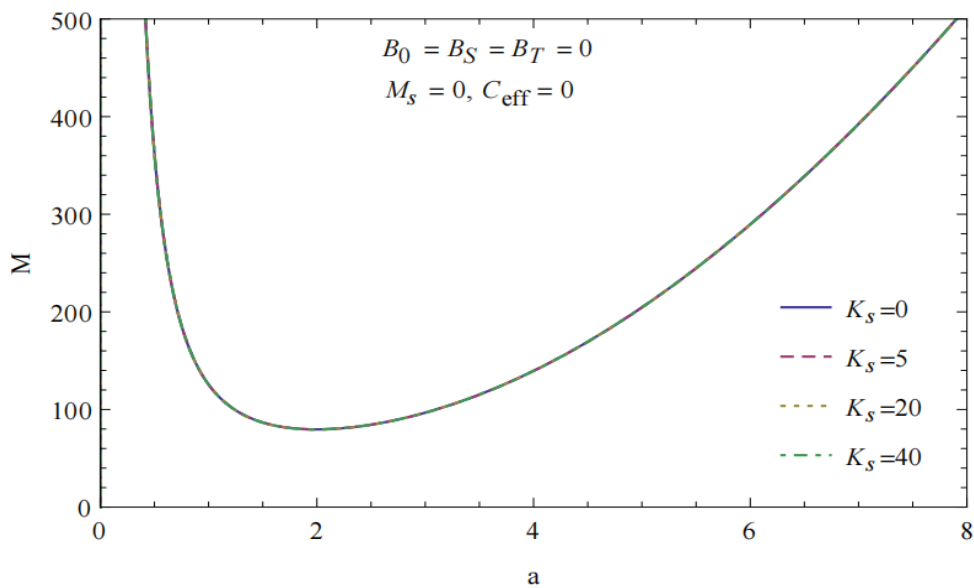


**Figure 7.** Numerically calculated Marangoni number versus the wave number ( $M_s = 0, C_{eff} = 0$ ).



Figures 2 and 3 demonstrate the variation of the critical Marangoni number  $M$  against the wave number  $\alpha$  under the influence of  $B_0$ ,  $B_T$ ,  $B_S$ ,  $M_s$ ,  $C_{eff}$ ,  $K_s$ , and  $K_t$ . It is now clear that as the wave number increases, the Marangoni number decreases and attains its minimum value  $M_c$ , a critical Marangoni number. After attaining its minimum value, it starts increasing. It is now clear that the effect of increasing the values of  $K_f$  is to increase the value of  $M_c$  and its effect is to stabilize the fluid and delays the onset of convection. It is also clear that when  $K_f = 0$ , we can reproduce the result obtained by Boeck and These [3]. Also, it is evident from these plots the effect of increasing the value of  $M_s$  is to decrease the value of the critical Marangoni number  $M_c$  and its effect is to enhance heat transfer and advance the onset of convection. In the case of effective Crispation number  $C_{eff} = 0$ , that is, for a non-deformable free surface, the controller gain stabilizes the system. As  $C_{eff}$  increases its effect to decrease the value of  $M_c$  hence it advances the onset of convection when  $C_{eff}$  is large the long wavelength instability  $C_{eff}$  is even closer to these plots.

Figures 4 and 5 shows the variation of Marangoni number as a function of wave number when  $C_{eff} = 0.001$ , when  $B_i = B_o = 0$  for the range value of  $K_t$ . The situation is significantly different for the case  $C_{eff} = 0$  (figure2). At  $\alpha = 0$ , the Critical Marangoni number is zero, and there is only the conduction state of the system. It is evident from Figures 6 and 7 that the increase of  $K_s$  does not affect the Marangoni number, and its effect is almost negligible even with the increase of the effective Crispation number. Table 1, Table 2, and Table 3 show the Tabulation of different values of critical Marangoni number and wave number for different parameters.

**Table 1.** Tabulation of critical Marangoni number and wave number for different parameters.

$M_s$	$B_0, B_t=0$		$K_s, K_t=0$		$C_{eff} = 0$		$C_{eff} = 0.001$		$C_{eff} = 0.002$	
	$M_c$	$a_c$	$M_c$	$a_c$	$M_c$	$a_c$	$M_c$	$a_c$	$M_c$	$a_c$
0	79.6067	1.9929	78.4757	1.94673	77.2778	1.8948				
25	54.6067	1.9929	53.4757	1.94673	52.2778	1.8948				
50	29.6067	1.9929	28.4757	1.94672	27.2778	1.8948				

**Table 2.** Tabulation of critical Marangoni number and wave number for different parameters.

$M_s$	$B_0, B_t=0$		$C_{eff} = 0.001$		$K_s = 5$		$K_t = 0$		$K_t = 5$		$K_t = 20$		$K_t = 40$	
	$M_c$	$a_c$	$M_c$	$a_c$	$M_c$	$a_c$	$M_c$	$a_c$	$M_c$	$a_c$	$M_c$	$a_c$	$M_c$	$a_c$
0	144.084	3.0072	144.084	3.0072	144.084	3.0072	144.084	3.0072	144.084	3.0072	144.084	3.0072	144.099	3.0072
25	105.064	2.7287	119.084	3.0072	131.301	3.0921	136.339	3.0786						
50	60.7892	2.3619	94.0837	3.0072	118.014	3.1879	128.320	3.1622						

**Table 3.** Tabulation of critical Marangoni number and wave number for different parameters.

$M_s$	$B_0, B_t=0$		$C_{eff} = 0.001$		$K_t = 20$		$K_s = 0$		$K_s = 2$		$K_s = 4$		$K_s = 5$	
	$M_c$	$a_c$	$M_c$	$a_c$	$M_c$	$a_c$	$M_c$	$a_c$	$M_c$	$a_c$	$M_c$	$a_c$	$M_c$	$a_c$
0	78.4572	1.94673	111.033	2.54174	134.191	2.8761	144.084	3.0072						
25	74.2881	2.01417	102.791	2.63025	122.781	2.9641	131.301	3.0921						
50	69.8871	2.10319	94.1486	2.73818	110.972	3.0656	118.142	3.1879						

#### 4. Conclusions

The effect of the control on the onset of Surface-tension driven convection in a horizontal Newtonian fluid in the presence of a uniform internal heat source is investigated. The analytical expression for the thermal Marangoni number is obtained as a function of the



parameter of the problem. It is shown that effect of the controller  $K_t$  is to delay the onset of convection and stabilize the system in the case of a non-deforming surface. But  $K_s$  Has negligible effect. However, the controller gain is not effective in the case of a deforming surface. We have shown that the effect of the Crispation number is to destabilize the system.

## Funding

This research received no external funding.

## Acknowledgments

The Authors thank the Management and Principal KLE S. Nijalingappa College and Ramaiah Institute of Technology, Bengaluru, Karnataka, for providing facilities to carry out this research work.

## Conflicts of Interest

The authors declare no conflict of interest.

## References

1. Ramachandramurthy, V.; Aruna, A.S.; Kavitha, N. Bénard–Taylor Convection in Temperature-Dependent Variable Viscosity Newtonian Liquids with Internal Heat Source. *International Journal of Applied and Computational Mathematics* **2020**, *6*, 1-14, <https://doi.org/10.1007/s40819-020-0781-1>.
2. Aruna, A.S. Non-linear Rayleigh–Bénard magnetoconvection in temperature-sensitive Newtonian liquids with heat source. *Pramana* **2020**, *94*, 1-10, <https://doi.org/10.1007/s12043-020-02007-7>.
3. Chandrasekhar, S. *Hydrodynamic and Hydromagnetic Stability*. International Series of Monographs on Physics. Clarendon Press, Oxford, **1961**.
4. Pearson, J.R.A. On convection cells induced by surface tension. *Journal of Fluid Mechanics* **1958**, *4*, 489-500, <https://doi.org/10.1017/S0022112058000616>.
5. Sparrow, E.M.; Goldstein, R.J.; Jonsson, V.K. Thermal instability in a horizontal fluid layer: effect of boundary conditions and nonlinear temperature profile. *Journal of Fluid Mechanics* **1964**, *18*, 513-528, <https://doi.org/10.1017/S0022112064000386>.
6. Roberts, P.H. Convection in horizontal layers with internal heat generation. Theory. *Journal of Fluid Mechanics* **1967**, *30*, 33-49, <https://doi.org/10.1017/S0022112067001284>.
7. Char, M.-I.; Chiang, K.-T. Stability analysis of Benard-Marangoni convection in fluids with internal heat generation. *Journal of Physics D: Applied Physics* **1994**, *27*, 748-755, <https://doi.org/10.1088/0022-3727/27/4/012>.
8. Wilson, S.K. The effect of uniform internal heat generation on the onset of steady Marangoni convection in a horizontal layer of fluid. *Acta Mechanica* **1997**, *124*, 63-78, <https://doi.org/10.1007/BF01213018>.
9. Aruna, A.S.; Kumar, V.; Basavaraj, M.S. The effect of temperature/gravity modulation on finite amplitude cellular convection with variable viscosity effect. *Indian Journal of Physics* **2022**, *96*, 2427-2436, <https://doi.org/10.1007/s12648-021-02172-4>.
10. Tang, I.; Bau, H.H. Stabilization of the no-motion state in Rayleigh-Benard convection through the use of feedback control. *Physical Review Letters* **1993**, *70*, 1795-1798, <https://doi.org/10.1103/PhysRevLett.70.1795>.
11. Tang, J.; Bau, H.H. Stabilization of the no-motion state in the Rayleigh–Bénard problem. *Proceedings of the Royal Society of London. Series A: Mathematical and Physical Sciences* **1994**, *447*, 587-607, <https://doi.org/10.1098/rspa.1994.0157>.
12. Howle, L.E. Linear stability analysis of controlled Rayleigh–Bénard convection using shadowgraphic measurement. *Physics of Fluids* **1997**, *9*, 3111-3113, <https://doi.org/10.1063/1.869428>.
13. Or, A.C.; Kelly, R.E.; Cortelezzi, L.; Speyer, J.L. Control of long-wavelength Marangoni–Bénard convection. *Journal of Fluid Mechanics* **1999**, *387*, 321-341, <https://doi.org/10.1017/S0022112099004607>.
14. Bau, H.H. Control of Marangoni–Bénard convection. *International Journal of Heat and Mass Transfer* **1999**, *42*, 1327-1341, [https://doi.org/10.1016/S0017-9310\(98\)00234-8](https://doi.org/10.1016/S0017-9310(98)00234-8).
15. Arifin, N.M.; Nazar, R.; Senu, N. Feedback of the Marangoni-Benard instability in a fluid layer with free-slip bottom. *Journal of Phys. Soc.* **2007**, *22*, 97–105.
16. Boeck, T.; Thess, A. Inertial Bénard–Marangoni convection. *Journal of Fluid Mechanics* **1997**, *350*, 149-175, <https://doi.org/10.1017/S0022112097006782>.

17. Basavaraj, M.S.; Shobha, T.; Aruna, A.S. The combined effect of porosity of porous media and longitudinal magnetic field on stability of the modified plane Poiseuille flow. *Sādhanā* **2021**, *46*, 1-10, <https://doi.org/10.1007/s12046-021-01739-5>.
18. Basavaraj, M.S.; Aruna, A.S.; Kumar, V.; Shobha, T. MHD instability of the pressure-driven plane laminar flow in the presence of the uniform coplanar magnetic field: Linear stability analysis. *Heat Transfer* **2021**, *50*, 5779-5792, <https://doi.org/10.1002/htj.22148>.
19. Basavaraj, M.S. Instability of the plane parallel flow through a saturated porous medium in the presence of a longitudinal magnetic field using the Chebyshev collocation method. *International Journal of Non-Linear Mechanics* **2021**, *137*, <https://doi.org/10.1016/j.ijnonlinmec.2021.103828>.
20. Sequeira, Y.; Maitra, A.; Pandey, A.; Jung, S. Revisiting the NASA surface tension driven convection experiments. *npj Microgravity* **2022**, *8*, <https://doi.org/10.1038/s41526-022-00189-5>.
21. Ramachandraiah, M.; Basavaraju, S. The Onset of Buoyancy and Surface Tension Driven Convection in a Ferrofluid Layer by Influence of General Boundary Conditions. *Open Journal of Fluid Dynamics* **2022**, *12*, 56-68, <https://doi.org/10.4236/ojfd.2022.121003>.
22. Sumithra, R.; Arul, S.T. Single component Darcy-Benard surface tension driven convection of couple stress fluid in a composite layer. *Malaya Journal of Matematik* **2021**, <https://doi.org/10.26637/MJM0901/0140>.
23. Qin, P.; Sun, J.; Yang, X.; Wang, Q. Battery thermal management system based on the forced-air convection: A review. *eTransportation* **2021**, *7*, 2590-1168, <https://doi.org/10.1016/j.etrans.2020.100097>.
24. Samrat, S.P.; Reddy, M.G.; Sandeep, N. Buoyancy effect on magnetohydrodynamic radiative flow of Casson fluid with Brownian moment and thermophoresis. *The European Physical Journal Special Topics* **2021**, *230*, 1273-1281, <https://doi.org/10.1140/epjs/s11734-021-00043-x>.
25. Basavaraj, M.S.; Girinath Reddy, M.; Aruna, A.S.; Dinesh P.A. A nonlinear mixed convective oscillatory flow over a semi-infinite vertical plate through porous medium under uniform magnetic field. *Int. J. of Adv. Res.* **2020**, *8*, 308-321, <http://dx.doi.org/10.21474/IJAR01/11100>.
26. Ramachandramurthy, V.; Kavitha, N.; Aruna, A.S. The Effect of a Magnetic Field on the Onset Of Bénard Convection in Variable Viscosity Couple-Stress Fluids Using Classical Lorenz Model. *Appl Math.* **2021**, *67*, 509-523, <https://doi.org/10.21136/AM.2021.0010-21>.
27. Aruna, A.S.; Kumar, V.; Basavaraj, M.S. The effect of temperature/gravity modulation on finite amplitude cellular convection with variable viscosity effect. *Indian Journal of Physics* **2022**, *96*, 2427-2436, <https://doi.org/10.1007/s12648-021-02172-4>.
28. Khashi'ie, N.S.; Waini, I.; Kasim, A.R.M.; Zainal, N.A.; Arifin, N.M.; Pop, I. Thermal progress of a non-Newtonian hybrid nanofluid flow on a permeable Riga plate with temporal stability analysis. *Chinese Journal of Physics* **2022**, *77*, 279-290, <https://doi.org/10.1016/j.cjph.2022.03.019>.
29. Dzulkifli, N.F.; Bachok, N.; Yacob, N.A.; Arifin, N.M.; Rosali, H.; Pop, I. Thermal radiation on mixed convection heat and mass transfer over a vertical permeable stretching/shrinking sheet with Soret and Dufour effects. *Journal of Engineering Mathematics* **2021**, *132*, <https://doi.org/10.1007/s10665-021-10188-2>.
30. Abu Bakar, S.; Md Arifin, N.; Khashi'ie, N.S.; Bachok, N. Hybrid Nanofluid Flow over a Permeable Shrinking Sheet Embedded in a Porous Medium with Radiation and Slip Impacts. *Mathematics* **2021**, *9*, <https://doi.org/10.3390/math908087>.
31. Khashi'ie, N.S.; Arifin, N.M.; Pop, I. Non-Darcy mixed convection of hybrid nanofluid with thermal dispersion along a vertical plate embedded in a porous medium. *International Communications in Heat and Mass Transfer* **2020**, *118*, <https://doi.org/10.1016/j.icheatmasstransfer.2020.104866>.
32. Ghasemi, S.E.; Hatami, M. Solar radiation effects on MHD stagnation point flow and heat transfer of a nanofluid over a stretching sheet. *Case Studies in Thermal Engineering* **2021**, *25*, <https://doi.org/10.1016/j.csite.2021.100898>.
33. Mathew, A.; Areekara, S.; Sabu, A.S.; Saleem, S. Significance of multiple slip and nanoparticle shape on stagnation point flow of silver-blood nanofluid in the presence of induced magnetic field. *Surfaces and Interfaces* **2021**, *25*, <https://doi.org/10.1016/j.surfin.2021.101267>.